Talanta 143 (2015) 344–352

Contents lists available at ScienceDirect

Talanta

journal homepage: www.elsevier.com/locate/talanta

Determination of Sudan I in paprika powder by molecularly imprinted polymers–thin layer chromatography–surface enhanced Raman spectroscopic biosensor

Fang Gao [a,b], Yaxi Hu [a], Da Chen [c], Eunice C.Y. Li-Chan [a], Edward Grant [b], Xiaonan Lu [a,*]

[a] Food, Nutrition, and Health Program, Faculty of Land and Food Systems, The University of British Columbia, Vancouver, British Columbia, Canada V6T 1Z4
[b] Department of Chemistry, The University of British Columbia, Vancouver, British Columbia, Canada V6T 1Z1
[c] State Key Laboratory of Precision Measuring Technology and Instruments, Tianjin University, Tianjin 300072, China

ARTICLE INFO

Article history:
Received 21 March 2015
Received in revised form
1 May 2015
Accepted 2 May 2015
Available online 9 May 2015

Keywords:
Molecular imprinting
Raman spectroscopy
Separation
Food safety
Multivariate analysis

ABSTRACT

Sudan I is a carcinogenic and mutagenic azo-compound that has been utilized as a common adulterant in spice and spice blends to impart a desirable red color to foods. A novel biosensor combining molecularly imprinted polymers (MIPs), thin layer chromatography (TLC) and surface enhanced Raman spectroscopy (SERS) could determine Sudan I levels in paprika powder to 1 ppm (or 2 ng/spot). Sudan I spiked paprika extracts (spiking levels: 0, 1, 5, 10, 40, 70 and 100 ppm) were prepared. Sudan I imprinted polymers were synthesized by employing the interaction between Sudan I (template) and methacrylic acid (functional monomer), followed by washing to remove Sudan I leaving the Sudan I-binding sites exposed. MIPs were used as a stationary phase for TLC and could selectively retain Sudan I at the original spot with little interference. A gold colloid SERS substrate could enhance Raman intensity for Sudan I in this MIP–TLC system. Principal component analysis plot and partial least squares regression (R^2=0.978) models were constructed and a linear regression model (R^2=0.983) correlated spiking levels (5, 10, 40, 70 and 100 ppm) with the peak intensities (721 cm^{-1}) of Sudan I SERS spectra. Both separation (30–40 s) and detection (1 s or 0.1 s) were extremely fast by using both commercial bench-top and custom made portable Raman spectrometers. This biosensor can be applied as a rapid, low-cost and reliable tool for screening Sudan I adulteration in foods.

1. Introduction

As an industrial dye, Sudan I is commonly used to color oils, waxes, and polishes. It is also added illegally to foodstuffs and cosmetics for color enhancement [1]. The compound is classified as a carcinogenic and mutagenic compound by International Agency for Research on Cancer [1]. In July 2003, Sudan I was detected in chili products imported from India by a French lab, and European community immediately released the legislation to track and remove the contaminated food products [2]. In February 2005, the United Kingdom recalled more than 470 food products contaminated with Sudan I [3]. A large adulteration incident with Sudan I spread globally later in the same year, causing tremendous panic and concern over food safety [3]. Monitoring Sudan I in foods is required due to the wide adulteration of this azo compound in a variety of natural agricultural products and processed foods, and rapid, low-cost, reliable and high-throughput methods are in high demand.

Chromatographic methods coupled with various detectors for the detection of Sudan I have been studied [2,4]. Liquid chromatography [5] has validated to be essential as a separation method because Sudan I is thermally unstable, making gas chromatography (GC) inappropriate without derivatization [6]. The complexity of typical food samples demands a long column running time (15 min or more) for separation; thus, LC is not suitable for rapid detection. In terms of detectors, UV–vis spectrometry [7] lacks specificity and leads to misidentification of analytes [2]. Mass spectrometry (MS) is substantially more reliable and shows a good limit of detection (LOD). Atmospheric pressure chemical ionization tandem MS combining isotope dilution was used to assay Sudan I in food samples with sensitivity (LOD of Sudan I in food extract: 0.025 ppm) 20 times better than that of a high-performance liquid chromatography (HPLC)-UV approach [2]. He et al. [6] performed GC–MS approach under electron impact mode or negative chemical ionization mode to determine Sudan I in eggs with an LOD of 2.0–2.1 μg/kg. However, MS is well-known as an expensive detector. In sum, column-based chromatographic approaches were

* Corresponding author. Tel.: +1 604 822 2551; fax: +1 604 822 5143.
E-mail address: xiaonan.lu@ubc.ca (X. Lu).

http://dx.doi.org/10.1016/j.talanta.2015.05.003
0039-9140/

time-consuming and sometimes expensive (*i.e.* MS), resulting in less preference.

Alternatively, TLC or high-performance TLC (HPTLC) for the detection of Sudan I has been studied as well. Quantitative study of the analyte zone on a TLC plate often involves scraping the stationary phase off the plate and extracting the analyte from the sorbent in multiple steps. Unfortunately, this may cause loss of analyte at each step, and requires a further off-line detection by either MS [5] or nuclear magnetic resonance [7]. Having an effective interface between plate and detector is needed [8]. To avoid the loss and achieve on-line detection, Kandler et al. [9] developed a fast and low-cost HPTLC-densitometry approach to determine Sudan I in food products. The LOD of this method was 30–150 ng/zone, but they realized the limited reliability of this approach due to sample matrix effect. In terms of stationary phase of the chromatographic approaches, reverse phase C_{18} were most common [2,4,6]. Further, a novel stationary phase (*i.e.* MIPs) to extract Sudan I from food samples has recently been developed [10–12]. MIPs are often regarded as an "artificial antibody" because MIPs can form "lock and key" bonds with specific template molecules. The precursor (*i.e.* the newborn monomer derived from the interaction between a functional monomer and a template molecule) copolymerizes with a cross-linking monomer (*i.e.* monomer which serves to provide MIPs rigidity) to produce durable template-imprinted polymers. After the removal of the template, the specific binding sites on MIPs are exposed and available for selective rebinding of the template from a complex sample matrix, such as foods. Functional monomers, cross-linking monomers, initiators, solvents and other parameters vary according to different template molecules. MIPs are widely used for separation and determination of the analytes in complicated samples [13,14]. Previous studies demonstrated that MIPs towards Sudan I were generated and packed either into solid phase extraction (SPE) cartridges [15] or HPLC analytical columns [16] or pre-columns [10] for separation, with a pre-treatment (*e.g.* solid–liquid extraction (SLE)) required for real samples. However, column conditioning is time consuming and sometimes expensive detectors are required.

Sudan I has been analyzed without chromatographic separation. For example, Lopez, [17] Di Anibal [18] and Cheung [3] individually conducted SLE and SERS detection of Sudan I in food samples, applying multivariate analysis as a screening tool. The LOD of these approaches were 10^{-7} M (Sudan I in extract) and 48 μg/kg (Sudan I in chili powder), respectively. In addition, electrochemical [*e.g.* carbon electrode modified by silver nanoparticles-graphene [19] or multi-walled carbon nanotubes (MWNTs) [20] and ionic liquid coupled with MWNTs [21]] and chemiluminescence (*e.g.* quenched fluorescence of quantum dots [22]) measurements can also be applied to determine Sudan I in food samples, but intensive sample pre-treatment was required.

As a derivative of vibrational spectroscopy, SERS offers extremely low LOD and is capable of qualitative and quantitative analysis. It is known as a fast, cost-effective and non-destructive detection tool [23]. SERS is used to substitute normal Raman mode due to the weak intensity of Raman scattering signals of molecules, with only 1 out of 10 million of the scattered photons experiencing Raman scattering when incident light interacts with the target molecules. Nanoparticles or nanoscale roughened surface of metals (*e.g.* gold, silver and copper) can be employed as a SERS substrate to enhance the normal Raman signals of molecules. Enhancement effect is contributed by two factors: chemical enhancement caused by charge transfer between the molecule and the substrate, and electromagnetic enhancement when the molecule is placed in the zone of localized surface plasmon resonance of SERS substrate. The distance between the molecule and surface of substrate should be less than 10 nm [24]. Total enhancement factor can exceed 10^{14} and molecules can be easily distinguished due to their unique SERS spectral pattern [25]. Extensive research with analytes in foods by SERS have been conducted over the past several years [26]. Tip enhanced Raman scattering [27] and plasmon enhanced Raman scattering [28] are also rapidly developing because of the favor in single molecule detection. However, intensive sample pre-treatment was required to reduce sample matrix effect before the detection of trace level of chemical contaminants in foods by SERS. Otherwise, the detector of Raman instrument [*e.g.* charge-coupled device (CCD)] will record Raman signals of all the molecules in a sample.

We have developed novel MIPs–SERS biosensors to determine alpha-tocopherol [29], melamine [30] and chloramphenicol [31] in foods. MIPs were packed into SPE cartridges to separate analytes from food samples with minimum sample pre-treatment. Silver dendrite was used as SERS substrate to enhance Raman signal intensity improving sensitivity. Xue et al. [41] have integrated MIPs and SERS substrate to generate surface-imprinted core–shell Au nanoparticles which can selectively detect bisphenol A in water and drinks. Low-cost, rapid and reliable features of these biosensors were developed.

Compared to aforementioned column-based chromatographic methods, TLC requires less time for separation. TLC coupled with SERS has been explored for on-line, sensitive and cost-effective detection of chemicals in complex sample matrix [24,32–34]. Ultra-thin layer chromatography was developed by laser ablating silver onto a plate substrate to generate an ultra-thin film of silver that is capable of separating a mixture of a few dyes and enhancing the corresponding Raman signals [24]. Freye et al. [32] cured polydimethylsiloxane (PDMS) polymers in a mold as the solid phase extractor and physically deposited silver nanoparticles onto the top of PDMS to receive separated compounds transferred from a C_{18} silica gel TLC plate. SERS spectra of the separated compounds were recorded. Malachite green isothiocyanate, Rhodamine 6G, methylene violet, known as SERS active molecules[24,32], were used to test the performance of TLC–SERS, and the mixture of a few standard amino acids [34] was also tested; in addition, detection of aromatic pollutants in water by TLC–SERS has been reported as well [42]. Real samples were investigated, but sample pre-treatment was necessarily complex because these samples contained significant interferences [33]. Although TLC–SERS technique is sometimes a feasible approach to determine analytes in real samples rapidly, the sensitivity is low, separation still takes a couple of minutes [32].

Therefore, the objective of our current study was to develop an MIPs–TLC–SERS biosensor by using MIPs as the stationary phase of a TLC plate. To the best of our knowledge, this was the first study of an integrated MIPs–TLC–SERS biosensor to determine trace levels of food chemical hazards. We confirmed that the pre-treatment of food samples was simplified and TLC development was extremely fast (30–40 s) due to the "lock and key" principle between MIPs and Sudan I. Gold colloid was used to enhance Raman signals of Sudan I and the enhancement factor was $\sim 4 \times 10^4$. The lowest content of Sudan I in paprika powder that can be detected was 1 ppm. By using a portable Raman spectrometer, in-field and on-line detection of Sudan I contamination in paprika powder could be realized.

2. Materials and methods

2.1. Reagents

Sudan I, methacrylic acid (MAA), ethylene glycol dimethylacrylate (EGDMA), azobisisobutyronitrile (AIBN), chloroauric acid ($HAuCl_4$), trisodium citrate dihydrate, and acetonitrile (all in HPLC

grade) were purchased from Sigma-Aldrich (St. Louis, MO). Methanol, hexane, chloroform (all in HPLC grade) and acetic acid were purchased from Fisher Scientific (Waltham, MA). Paprika powders (2 brands: paprika 1 and paprika 2) were obtained from different local grocery stores in Vancouver, British Columbia, Canada. Deionized (DI) water at 18.2 MΩ/cm was prepared by the Millipore system (Billerica, MA). The stock solution of Sudan I at 1000 ppm in acetonitrile was prepared.

2.2. Synthesis and characterization of MIPs

The template Sudan I (0.3 mmol), functional monomer MAA (1.2 mmol), cross-linking monomer EGDMA (8 mmol) were mixed with methanol (3 mL) and chloroform (0.5 mL) in a glass vial. The mixture was sonicated for 10 min. The initiator AIBN (20 mg) was added, and the whole mixture was purged by N_2 for 5 min. The polymerization was thermally initiated at 55 °C for 20 h (Fig. S1). Polymer was ground and sieved by a 200 mesh. MIPs in powder form (<75 μm) were washed with methanol and acetic acid (9:1, v/v) to remove template by monitoring UV–vis signal of Sudan I at 483 nm. Another wash by methanol was carried out to remove acetic acid. MIPs were dried under vacuum for 4 h. Non-imprinted polymers (NIPs) were prepared in the same manner without the addition of Sudan I.

Rebinding assay was conducted to evaluate the specific binding ability of MIPs to Sudan I. Static studies were performed by re-exposing 20 mg MIPs powder (or NIPs powder) to 2 mL Sudan I solution in acetonitrile and water (1:1, v/v) at 22 °C for 3 h. The concentrations of Sudan I solutions used were 5, 10, 20, 30 and 45 ppm, respectively. Supernatants were collected and centrifuged (2348*g*, 5 min). UV–vis spectra (483 nm) were acquired to determine the concentrations of analyte in the supernatants. Kinetic studies were performed by suspending 100 mg MIPs powder (or NIPs powder) to 10 mL Sudan I solution at 10 ppm. At each time point (1, 5, 10, 20, 30, 60, 90 and 120 min), 1 mL mixture was collected and centrifuged (2348 × *g*, 5 min), and the supernatant was measured for the unbound template molecules by UV spectrometry at 483 nm.

2.3. Pre-treatment of paprika samples

Sudan I stock solution (1000 ppm) was spiked into paprika powder (0.1 g). Different amount of the stock solution (0, 2, 10, 20, 80,140 and 200 μL) was mixed with untreated powder, and acetonitrile was added accordingly to make the total volume of Sudan I solution in each sample to 200 μL. These artificially contaminated paprika samples were then mixed with 1.82 mL of acetonitrile to the spiking levels of 0, 1, 5, 10, 40, 70 and 100 ppm, respectively, followed by sonication for 10 min to extract Sudan I. The extracts were centrifuged (2348*g*, 5 min) and filtrated. Concentrations of Sudan I in the extracts were determined by HPLC (Agilent 1100 series, Germany) equipped with a quaternary pump and a diode array detector. Column conditions were described in Fig. S4.

2.4. Synthesis of gold (Au) colloid

Au colloid was synthesized following the protocol by Cheung and coauthors [3]. $HAuCl_4$ (1 mM, 50 mL) was brought to boil first, and sequentially reduced by trisodium citrate (38.8 mM, 5 mL). The mixture was kept boiling for 30 min. Both pH and UV–vis spectrum were recorded after the mixture was chilled down. Gold colloid with a wine red color was ready to be used.

2.5. Fabrication of MIPs–TLC plate and developing

MIPs powder (50 mg) was suspended in 0.5 mL DI water and 0.1 mL ethanol thoroughly. The slurry was spread on a clean glass slide with dimension of 25 mm × 75 mm and dried at 22 °C for 4 h. The thickness of the sorbent was controlled between 0.35 and 0.40 mm. TLC plate developing was followed by the conventional way: spotting (2 μL paprika extract), developing and drying. Hexane and chloroform (1:1, v/v) were used as the optimal developing solvent.

2.6. SERS detection of Sudan I in paprika extract and data analysis

Au colloid (12 μL for bench-top Raman spectrometer or 20 μL for portable Raman spectrometer) was applied onto the original spot. The laser was introduced immediately onto the original spot and Raman spectra were acquired. Both bench-top Raman spectrometer (Renishaw, Gloucestershire, UK) and portable Raman spectrometer (custom made) were set up for spectral collection.

Near infrared laser (785 nm, 25 mW) was equipped with bench-top Raman spectrometer, coupled with 1200 groove/mm grating to disperse scattered photons and a 578 by 385 pixel CCD array detector to convert those photons to electronic form as read out. Raman spectral scan was conducted by a 50 × Nikon objective (NA=0.75, WD=0.37 mm) of an optical microscope with a movable sample stage in *x*–*y*–*z* dimension (Leica Biosystems, Germany). Spectrum range of either 350–1650 cm^{-1} (10 s exposure time) or 703–1262 cm^{-1} (1 s exposure time) were selected.

Raman spectra were also recorded using the portable Raman system with a backscattering probe, with dimension of 127 × 165 × 51 mm^3 and weight of 1.2 kg (Fig. 6). The instrument uses a 785 nm single-mode diode laser source with a power of 100 mW for illumination. The backscattered light was collected with free-space design, and a Volume-Phase Holographic grating disperses this light over an image plane measured in CCD pixels as 64 high × 1024 width, providing 1024 pixel number spanning a Raman shift interval from 200–2200 cm^{-1}. Each Raman spectrum was collected in 0.1 s and each data point was acquired at every 3 cm^{-1}.

WiRE v3.4 was programmed for spectral collection and initial processing (*e.g.* baseline correction). Further data analysis and construction of chemometric models were performed in Delight 3.2.1 (D-Squared Development Inc., LaGrande, OR, USA). The wavenumbers of 740–1190 cm^{-1} in 703–1262 cm^{-1} dataset (1 s exposure time) were negated for model development, whereas 710–725 cm^{-1} and 1210–1235 cm^{-1} were selected for chemometric analysis of the dataset of 350–1650 cm^{-1} (10 s exposure time).

Unsupervised principal component analysis (PCA) was conducted to reveal the variations among samples without a priori knowledge. Partial least squares regression (PLSR) model was constructed to predict sample concentration for sets of paprika powder samples spiked with different concentrations of Sudan I [35]. PLSR models were tested using leave-one-out cross-validation and 5 latent variables were selected. Root-mean-square error of cross-validation (RMSECV), root-mean-square error of prediction (RMSEP) and predictive squared correlation coefficient (Q^2) were calculated based on the training dataset from paprika 1 and the testing dataset from paprika 2, to assess the predictive capability of the developed PLSR models [36]. Equations are shown as below:

$$\mathrm{RMSECV} = \sqrt{\frac{\sum_{i}^{n} \left(c_i - \hat{c}_i\right)^2}{n}} \quad (1)$$

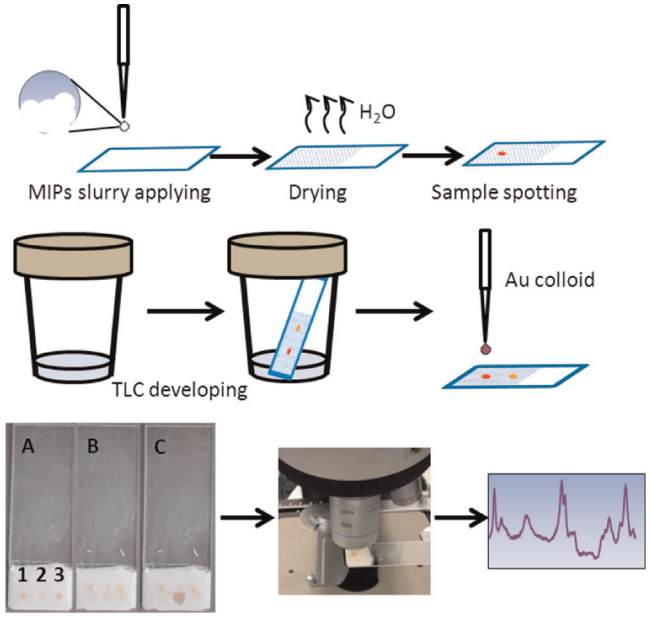

Fig. 1. Illustration of working mechanism of MIPs–TLC–SERS biosensor. (A: plate before developing, B: plate after developing, C: plated after addition of Au colloid; spot 1: 0 ppm Sudan I spike paprika extract, spot 2: 100 ppm Sudan I standard solution, spot 3: 100 ppm Sudan I spiked paprika extract.)

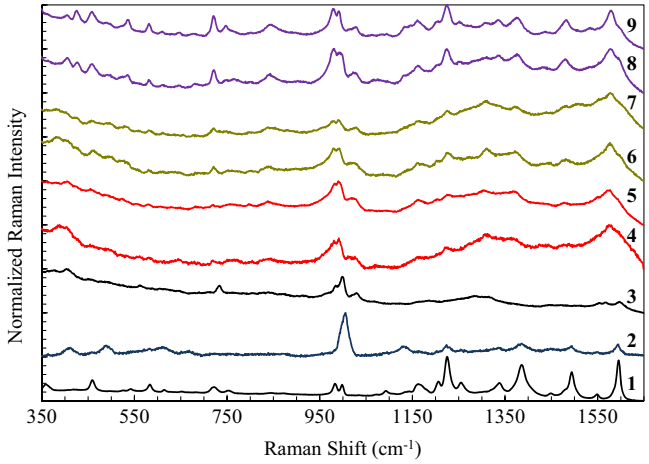

Fig. 2. Average SERS spectra of Sudan I (collected in 49 s) in the wavenumber range of 350–1650 cm^{-1}. [From bottom to top: normal Raman spectrum acquired from dried standard solution of 2 μL of 2000 ppm on clean glass slide (1), normal Raman spectrum from dried 2 μL of 1000 ppm of Sudan I standard solution on MIPs–TLC plate (2), SERS spectrum of 0 ppm (3) spiked paprika extract, 1 ppm (4) standard solution, 1 ppm (5) spiked paprika extract, 10 ppm (6) standard solution, 10 ppm (7) spiked paprika extract, 100 ppm (8) standard solution, 100 ppm (9) spiked paprika extract; SERS spectra were collected from the sample spots after MIPs–TLC developing; $n=8$ for each concentration.]

$$\mathrm{RMSEP} = \sqrt{\frac{\sum_{i}^{n}\left(c_i - \hat{c}_i\right)^2}{n}} \tag{2}$$

$$Q^2 = 1 - \frac{\sum_{i}^{n}\left(c_i - \hat{c}_i\right)^2}{\sum_{i}^{n}\left(c_i - \bar{c}_i\right)^2} \tag{3}$$

in which n is the number of samples (*i.e.* spectra), c_i is the real concentration of sample i, and $\hat{c}_i$ is the predicted concentration by models, while $\bar{c}_i$ is the arithmetic mean of all the testing dataset.

3. Results and discussions

3.1. Properties of MIPs

Rebinding assays were carried out to confirm the selectivity of MIPs towards Sudan I by comparing the performance of MIPs with control polymers (*i.e.* NIPs). A few parameters, such as imprinting factor (IF), adsorption capacity (Q) and the Scatchard plot model, were calculated and derived from the created isotherm based on the static studies [37]. Calculations of Q (Eq. 4), IF (Eq. 5) and formula of Scatchard plot (Eq. 6) are shown as follows:

$$Q = (C_i - C_f) \times V/W \tag{4}$$

$$\mathrm{IF} = Q_{\mathrm{MIPs}}/Q_{\mathrm{NIPs}} \tag{5}$$

$$Q/C_f = -Q/K_d + Q_{\max}/K_d \tag{6}$$

in which Q represents the adsorption capacity of MIPs or NIPs, C_i is the initial concentration of Sudan I before addition of polymer, C_f is the final concentration of Sudan I (in the supernatant) after rebinding, V is the volume of Sudan I solution (2 mL), and W represents the quantity of polymer (20 mg). In Eq. 6, K_d is the dissociation constant and $Q_{\max}$ represents the saturated adsorption capacity.

Along with the increase in initial concentration of Sudan I, Q_{MIPs} increased almost linearly compared to Q_{NIPs}, which expressed limitation at high concentrations [Fig. S2(A)]. Non-specific binding is the speculated factor to explain the similar values of Q_{NIPs} to Q_{MIPs} when the concentration of Sudan I was lower than 20 ppm. In comparison, differences between Q_{NIPs} and Q_{MIPs} in higher concentrations of Sudan I were significant ($P=0.01$) and this may be due to the imprinted binding sites that are specific to Sudan I on MIPs rather than NIPs. IF is usually used to evaluate the selectivity of MIPs towards template. It varies depending on the concentrations of analyte. At 45 ppm of C_i, IF was 1.46 [Fig. S2(A)]. We constructed the Scatchard plot of MIPs with a convex shape [Fig. S2(B)], in contrast, no similar plot pattern could be constructed using NIPs dataset. According to the theory of Scatchard plot [38], non-linear regression indicates the non-identical and dependent binding sites; in other words, binding at one site will affect the binding at another site, thus the plots indicate the different properties of MIPs and NIPs. Specific binding sites on MIPs have been discussed with the conclusion that they can be complementary to template in size, shape, and interactions [13] (*e.g.* covalent, H-bonding, hydrophobic). In the current study, H-bonding and size exclusion are the two major factors (Fig. S1). Thus, both physical and chemical elements contribute to specific binding. Taken together, binding sites on MIPs were specific towards Sudan I compared to NIPs.

Q_{MIPs} and Q_{NIPs} at different time points were plotted against the initial Sudan I concentration of 10 ppm for the kinetic studies. Instant binding and saturation were achieved within 5 min for control polymer (*i.e.* NIPs), while Q_{MIPs} gradually increased for the following 115 min although most binding was done for the first 5 min (Fig. S3). Different Q values of MIPs and NIPs after saturation and the time to reach saturation further validated the existence of specific binding sites on MIPs. Fast binding (86% in 5 min) was a good indicator for further TLC sample loading, in which potential loss could be limited.

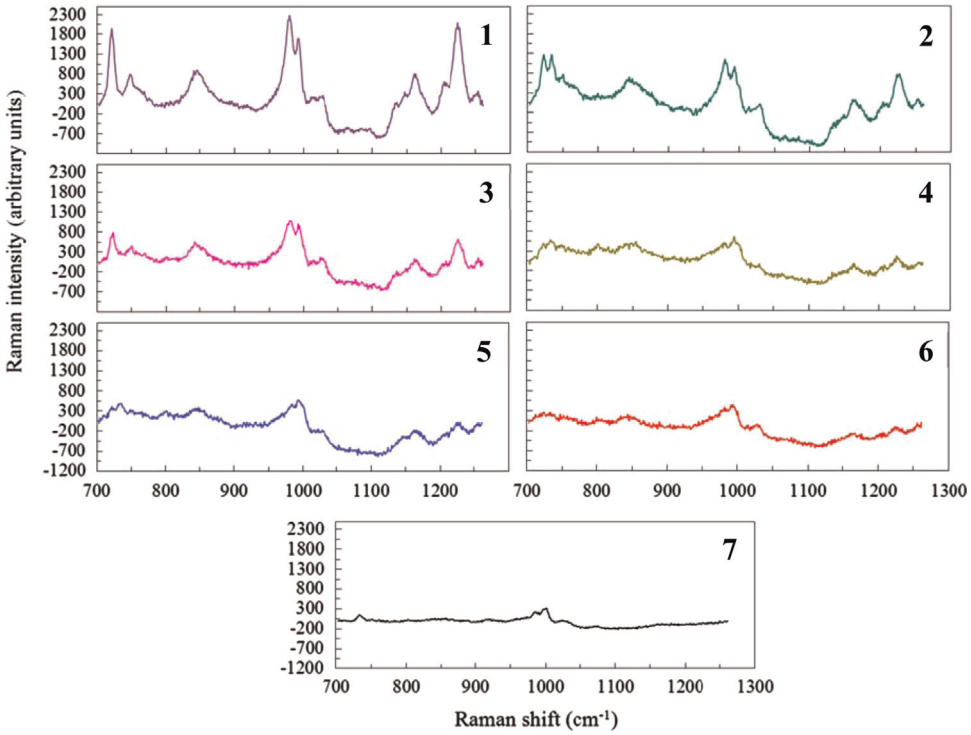

Fig. 3. Averaged SERS spectra of Sudan I (collected in 1 s) in the wavenumber range of 703–1262 cm^{-1}. [Sudan I spiked paprika extract: 0 ppm (7), 1 ppm (6), 5 ppm (5), 10 ppm (4), 40 ppm (3), 70 ppm (2) and 100 ppm (1); SERS spectra were collected from the sample spots after MIPs–TLC developing; $n=8$ for each concentration.]

3.2. Pre-treatment of food samples

Minimum sample treatment (*i.e.* SLE, 10 min by sonicating) was performed to extract Sudan I from paprika powder samples. In the meanwhile, unavoidable interferents were also extracted because of their solubility in acetonitrile. Recoveries were quantified by HPLC and are summarized in Table S1.

3.3. Synthesis of Au colloid

pH of Au colloid was 6.5 and UV–vis absorbance spectrum of Au colloid was shown in Fig. S5, in which the wavelength of maximum absorption was 525 nm. These parameters could be referred to further development of Au colloid in the same manner.

3.4. Fabrication of MIPs–TLC plate and developing

MIPs thickness and stationary phase area were optimized, given the fact that the gravity of sorbent may overcome friction between MIPs and glass slide, causing MIPs to fall off the plate during developing. Sample spotted within a small area was also desirable for further SERS detection. The amount of MIPs was optimized by using 50 mg and the thickness was controlled between 0.35 and 0.40 mm. A small portion of ethanol was added into the slurry for a better disperse of MIPs into liquid and avoiding generation of air bubbles. MIPs–TLC plate was ready to be used after it was completely dried under ambient temperature. Paprika extract (2 μL) was deposited to form a spot of ~3 mm in diameter and allowed to dry. For the developing, mixture of hexane and chloroform was selected without destroying the interaction between Sudan I and MIPs, but washing interferents away. The same MIPs–TLC plate at different developing stages is shown in Fig. 1. Spots on the plate (from left to right) indicated 0 ppm spiked extract, 100 ppm Sudan I standard solution in acetonitrile and 100 ppm spiked extract, respectively. Spiked extract showed more intensive color than the standard solution of Sudan I, indicating the massive components (as interferents) in the paprika samples. After developing, pale but visible red spots were left at the original spots but not 0 ppm spiked extract, indicating that Sudan I was successfully captured by MIPs.

Due to the selectivity of MIPs towards Sudan I, the retardation factor is not a concern because Sudan I in the extract was fixed at the original sample spot, whereas interferents moved upward with developing solvent. MIPs–TLC developing performance further validated the specific "lock and key" principle of MIPs towards Sudan I. In this case, developing time was shortened to be 30–40 s depending on the distance between sample spot and slide edge and less solvent was used.

3.5. SERS spectral acquisition and data analysis

After TLC developing, Au colloid was applied onto the original sample spot on MIPs–TLC plate. A preliminary experiment was conducted using different amounts of Au colloid for deposition and it was found that 12 μL of Au colloid could achieve a good enhancement of Sudan I Raman signal. Fig. 2 shows the SERS spectra of standard Sudan I and paprika extract spiked at different concentrations of Sudan I (after TLC developing). Bands in the 350–1650 cm^{-1} range could be seen in SERS spectra at 100 ppm (9) compared to the normal Raman spectrum of Sudan I (1) and the SERS spectra of Sudan I obtained by Cheung and coauthors [3], indicating the SERS spectra we acquired are indeed from Sudan I. Bands at 461, 581 and 721 cm^{-1} were significantly enhanced. Some band shifts existed, which may be attributed to the affinity between covalent bonds and Au colloid particles and physisorption strain [39]. Except bands assigned to Sudan I (Table S2), only limited interference bands appeared. Even at 1 ppm, bands at 461, 536, 581, 721, 980, 990,1224, 1377, 1482 and 1577 cm^{-1} (featured bands of Sudan I) were still distinct. In terms of SERS spectra from

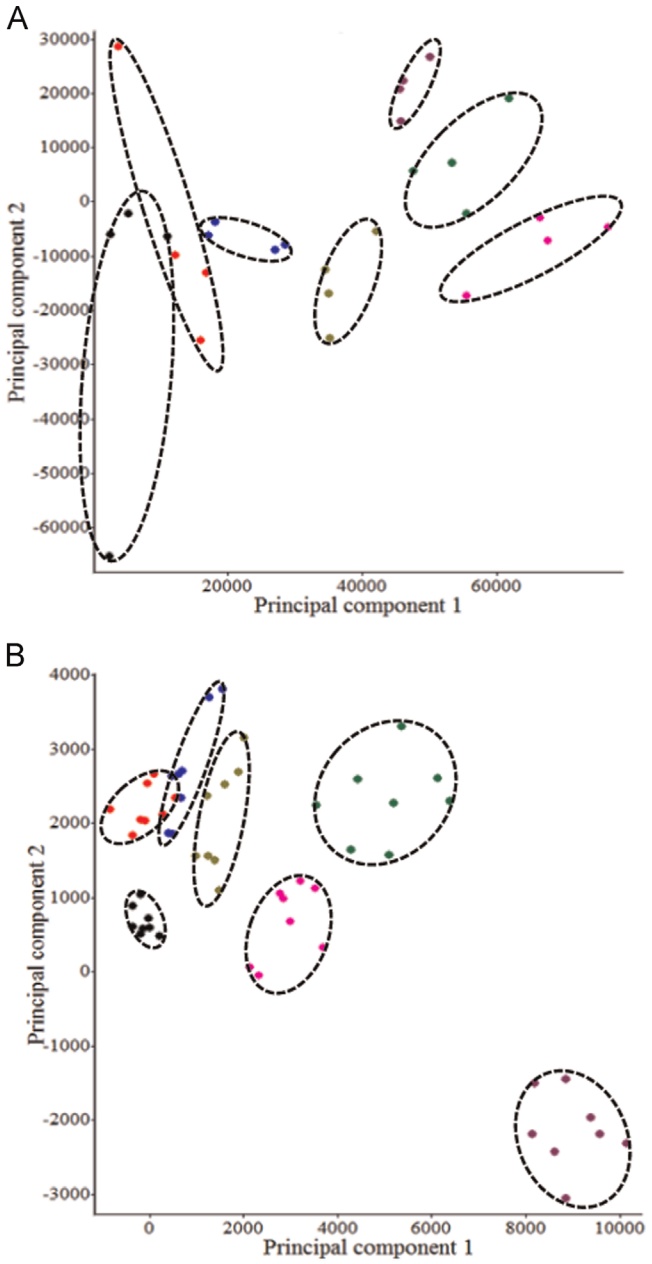

Fig. 4. Illustration of principal component analysis (PCA) models: (A) spectra in the wavenumber range of 350–1650 cm^{-1} (PC1: 57.4%, PC2: 34%; $n=4$ at each concentration); (B) spectra in the wavenumber range of 703–1262 cm^{-1} (PC1: 50%, PC2: 23.9%; $n=8$ at each concentration). [Sudan I spiked paprika extract: 0 ppm (black), 1 ppm (red), 5 ppm (blue), 10 ppm (olive), 40 ppm (pink), 70 ppm (green), 100 ppm (purple); SERS spectra were collected from the sample spots after MIPs–TLC developing.] ($n=5$). (For interpretation of the references to color in this figure legend, the reader is referred to the web version of this article.)

0 ppm spiked extract, no featured bands can be observed. Thus, good separation efficiency of MIPs–TLC plate was validated.

However, the developed MIPs–TLC plate had to be used for spectral collection immediately after the addition of Au colloid. SERS band intensity could not be maintained once the Au colloid was dried. It took 49 s for the collection of each SERS spectrum in the range of 350–1650 cm^{-1}. Collection of SERS spectra in the next cycle (another 49 s) or more resulted in a reduction of signal intensity. Time profiling was recorded with laser illuminated at a single spot on the plate (Fig. S6). Relative height (or peak area) of certain bands (*i.e.* 461, 721 and 1224 cm^{-1}) was reproducible, but not all bands within the first 49 s. Moreover, the reduction of band intensity was random, indicating the stringent time factor in terms of reliability of this MIPs–TLC–SERS biosensor. Aggregation of Au colloid particles during drying may account for the weaker SERS signal as the morphology of nanoparticles changed, resulting in the change of localized surface plasmon resonance; thus, enhancing ability of Au nanoparticles compromised accordingly [34].

Therefore, the ideal circumstance is to keep the Sudan I spot on MIPs in a dampened state. However, laser illumination generated heat and facilitated the drying of Au colloid. Faster spectral collection is thus the strategy to eliminate random reduction of SERS signal intensity. Compared to previous spectral collection in 49 s, the exposure time was shortened to 1 s with a narrow scanning wavenumbers (703–1262 cm^{-1}) due to the limitation of the bench-top Raman instrument. A few featured bands (*i.e.* 721, 980, 990, and 1224 cm^{-1}) could still be recorded in 50 s after the addition of Au colloid (Fig. 3).

Both univariate and multivariate analysis were conducted towards datasets of either short- or long-wavenumber range (703–1262 cm^{-1} or 350–1650 cm^{-1}) of Sudan I SERS spectra, aiming at testing the reproducibility and reliability of this MIPs–TLC–SERS biosensor. PCA plots were constructed to visualize spectral variations and leave-one-out cross-validation was employed to assess the performance of PLSR models. We also performed the linear regression towards the spectra with short wavenumber range (703–1262 cm^{-1}) as a comparison. In Fig. 4(A), the PCA plot of spectra with long wavenumber range (350–1650 cm^{-1}) was capable of differentiating high concentrations of spiked Sudan I, and the lowest concentration that could be clearly separated was 5 ppm. However, the coefficient of determination ($R^2=0.788$) of PLSR model [Fig. 5(A)] was not satisfactory. As we have discussed, the signal intensity of SERS spectra with 49 s collection time was strongly time dependent, indicating its inappropriate usage to quantify Sudan I. PCA plot of spectra with 1 s collection time [Fig. 4(B)] showed clear segregation clusters among most concentrations, with minor overlapping between the clusters of 1 ppm and 5 ppm. Corresponding PLSR model [Fig. 5(B)] also showed good linear regression ($R^2=0.978$).

Due to the challenge in separating 1 ppm and 5 ppm spiked Sudan I samples using PCA plot, we next created a linear regression model because we observed the trend of increasing peak intensity along with the increase in concentrations (spiking levels). Featured SERS band at 721 cm^{-1} was selected and a good linear correlation ($R^2=0.983$) was plotted between band intensity and corresponding concentration (spiking level) [Fig. 5(C)]. The prediction was conducted by incorporating one SERS spectrum of Sudan I at each spiked level in paprika 2 extract (*i.e.* the testing dataset) into the established models [Fig. 5(B) and (C)]. All the models established on the basis of 1 s collection time could validate the sensitivity and reliability of this biosensor. In terms of LOD, 1 ppm (or 2 ng/spot) was defined. The diameter of laser spot of bench-top Raman spectrometer on the MIPs–TLC plate is ~10 μm, whereas sample spot on plate showed 3 mm in diameter with 0.35–0.40 mm thickness. An even lower LOD could be achieved with a better manipulation of sample spot size and plate thickness.

We also performed silica gel TLC–SERS to determine Sudan I in paprika extract and compared it with the performance of MIPs–TLC–SERS. Standard solution of Sudan I (100 ppm) and 100 ppm Sudan I spiked paprika extract were used and sample spotting amount was 2 μL. However, it took 3.5 min for the separation (developing solvent: hexane/chloroform/acetic acid, 1:1:0.02 v/v) and no SERS signal could be recorded on the TLC plate whether it was wet or dry. This may be due to the inappropriate SERS substrate such as the size and morphology of nanoparticles or different types of colloids that are employed [40]. Parameters such as

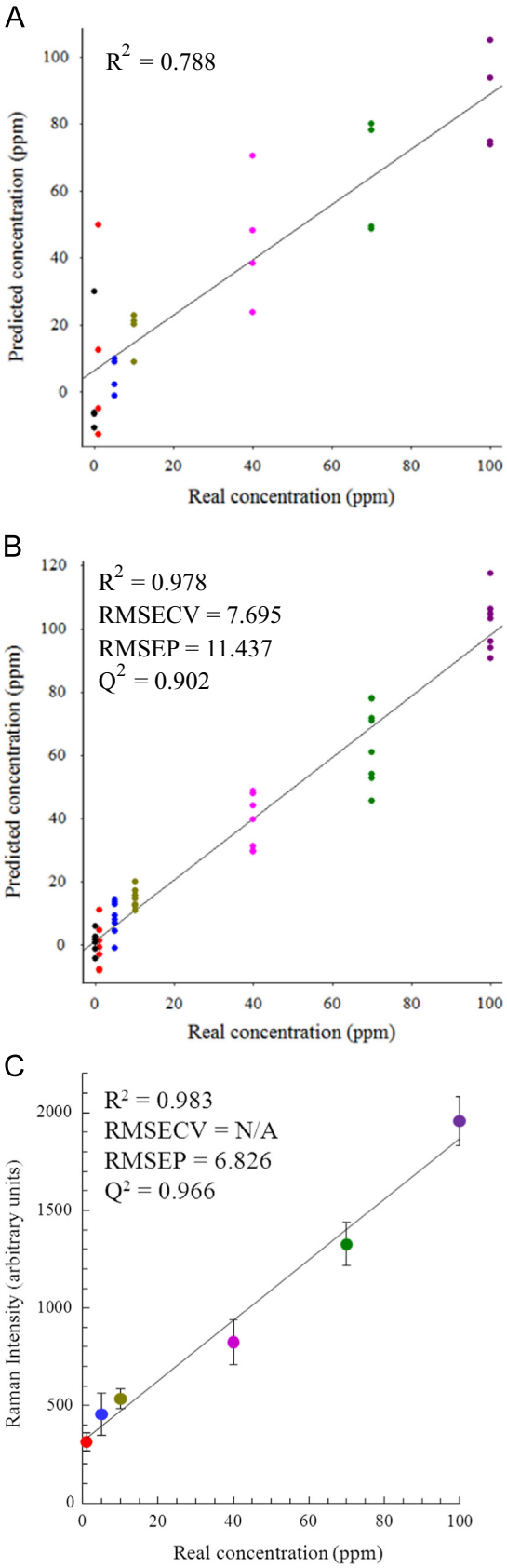

Fig. 5. Illustration of regression models: (A) established PLSR regression based on spectra in range of 350–1650 cm^{-1}; (B) established PLSR regression based on spectra in range of 703–1262 cm^{-1}; (C) establish linear regression based on band height at 721 cm^{-1} of spectra in range of 703–1262 cm^{-1} (values shown in: mean ± standard error of the mean, $n=8$ at each concentration.) [Sudan I spiked paprika extract: 0 ppm (black), 1 ppm (red), 5 ppm (blue), 10 ppm (olive), 40 ppm (pink), 70 ppm (green), 100 ppm (purple); SERS spectra were collected from the sample spots after MIPs–TLC developing.] (For interpretation of the references to color in this figure legend, the reader is referred to the web version of this article.)

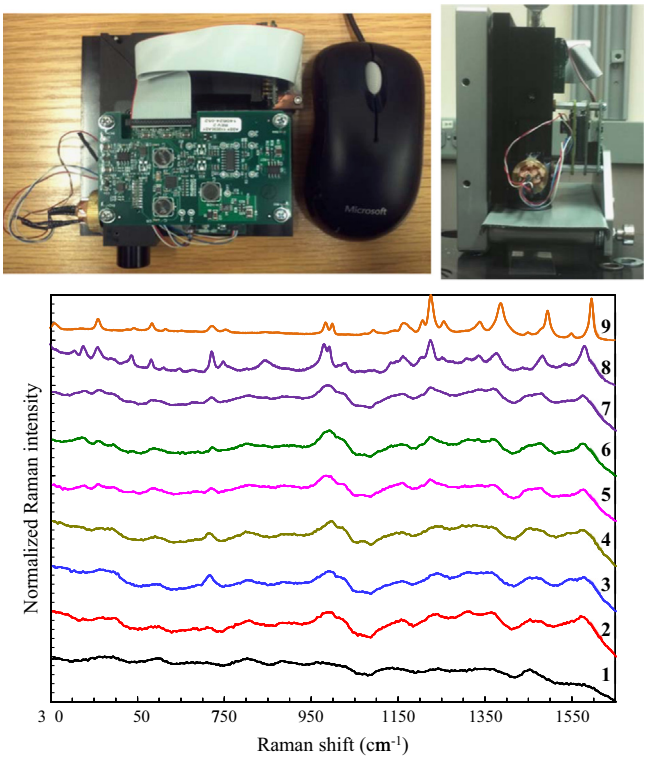

Fig. 6. Schematic illustration of SERS spectral collection by portable Raman spectrometer (top)and corresponding SERS spectral features of Sudan I in range of 350–1650 cm^{-1} (bottom). [From bottom to top: averaged SERS spectra ($n=3$) of Sudan I spiked paprika extract: 0 ppm (1), 1 ppm (2), 5 ppm (3), 10 ppm (4), 40 ppm (5), 70 ppm (6), 100 ppm (7); SERS spectra were collected by portable Raman spectrometer from the sample spots after MIPs–TLC developing. SERS spectrum of Sudan I spiked paprika extract from the sample spots after MIPs–TLC developing: 100 ppm (8) and normal Raman spectrum acquired from dried standard solution of 2 μL of 2000 ppm (9); spectra were collected by bench-top Raman spectrometer.]

separation time and LOD of these two approaches can be found in Table S3 and Fig. S7.

More Au colloid (20 μL) was applied to sample spot on the MIPs–TLC plate given the fact that laser power with 100 mW from portable Raman spectrometer can generate much higher thermal energy, resulting in challenges in spectral collection. Spectra collected from portable Raman spectrometer were averaged ($n=3$ at each concentration) and stacked in Fig. 6. Less resolution was founded due to the inherent properties of a portable instrument that tend to reduce sensitivity, but SERS spectra were still sufficient to assay the presence of Sudan I. Therefore, in-field or on-line screening of Sudan I can be conducted with a portable Raman spectrometer at least for screening purposes with further quantitative analysis performed by a bench-top Raman spectrometer.

4. Conclusions

We developed an innovative approach of MIPs–TLC–SERS to determine Sudan I in paprika powder. MIPs–TLC plate could separate Sudan I from paprika extract within 30–40 s with minimum sample pre-treatment required. Spectral collection by bench-top Raman spectrometer was finished in 1 s by adding Au colloid (as a SERS substrate) to a separated Sudan I spot on a TLC plate, aiming to obtain enhanced Raman spectra. The enhancement factor was $\sim 4 \times 10^4$, based on the calculation of peak height at 721 cm^{-1} after baseline correction of Sudan I spectra on MIPs–TLC plate. Chemometric and regression models showed that the detection of Sudan I was accurate and sensitive [LOD of 1 ppm (or 2 ng/spot)] using either bench-top or portable Raman spectrometer. This novel MIPs–TLC–SERS biosensor had fast, reliable and low cost features for in-field and on-line screening of food chemical contamination and adulteration.

Acknowledgement

This study was supported by funds award to X.L. by Natural Sciences and Engineering Research Council of Canada (NSERC RGPIN-2014-05487).

Appendix A. Supplementary information

Supplementary data associated with this article can be found in the online version at http://dx.doi.org/10.1016/j.talanta.2015.05.003

References

[1] N.A. Ahmed Refat, Z.S. Ibrahim, G.G. Moustafa, K.Q. Sakamoto, M. Ishizuka, S. Fujita, J. Biochem. Mol. Toxicol. 22 (2008) 77–84.
[2] L. Di Donna, L. Maiuolo, F. Mazzotti, D. De Luca, G. Sindona, Anal. Chem. 76 (2004) 5104–5108.
[3] W. Cheung, I.T. Shadi, Y. Xu, R. Goodacre, J. Phys. Chem. C 114 (2010) 7285–7290.
[4] T. Chiye, O. Takashi, O. Noriko, K. Hiroki, S. Kyoko, A. Hiroshi, K. Yoko, Am. J. Anal. Chem. 3 (2012) 570–575.
[5] M. Prosek, A. Golc-Wondra, I. Vovk, S. Andrensek, J. Planar Chromatogr. – Mod. TLC 13 (2000) 452–456.
[6] L. He, Y. Su, X. Shen, Z. Zeng, Y. Liu, Anal. Chim. Acta 594 (2007) 139–146.
[7] J.F. Nierengarten, C.O. Dietrich-Buchecker, J.P. Sauvage, J. Am. Chem. Soc. 116 (1994) 375–376.
[8] A.I. Gusev, O.J. Vasseur, A. Proctor, A.G. Sharkey, D.M. Hercules, Anal. Chem. 67 (1995) 4565–4570.
[9] H. Kandler, M. Bleisch, V. Widmer, E. Reich, J. Liq. Chromatogr. Relat. Technol. 32 (2009) 1273–1288.
[10] S. Wang, Z. Xu, G. Fang, Z. Duan, Y. Zhang, S. Chen, J. Agric. Food Chem. 55 (2007) 3869–3876.
[11] X.-Y. Xu, X.-G. Tian, L.-G. Cai, Z.-L. Xu, H.-T. Lei, H. Wang, Y.-M. Sun, Anal. Methods 6 (2014) 3751–3757.
[12] D. Ren, J. He, H. Zhang, Anal. Methods 6 (2014) 3079–3085.
[13] V. Pichon, J. Chromatogr. A 1152 (2007) 41–53.
[14] L.M. Kindschy, E.C. Alocilja, Biosens. Bioelectron. 20 (2005) 2163–2167.
[15] C. Baggiani, L. Anfossi, C. Giovannoli, Anal. Chim. Acta 591 (2007) 29–39.
[16] C. Allender, C. Heard, K. Brain, Chirality 9 (1997) 238–242.
[17] M.I. Lopez, I. Ruisanchez, M.P. Callao, Spectrochim. Acta A Mol. Biomol. Spectrosc. 111 (2013) 237–241.
[18] C.V. Di Anibal, L.F. Marsal, M.P. Callao, I. Ruisanchez, Spectrochim. Acta A Mol. Biomol. Spectrosc. 87 (2012) 135–141.
[19] E. Prabakaran, K. Pandian, Food Chem. 166 (2015) 198–205.
[20] D. Yang, L. Zhu, X. Jiang, J. Electroanal. Chem. 640 (2010) 17–22.
[21] Z. Mo, Y. Zhang, F. Zhao, F. Xiao, G. Guo, B. Zeng, Food Chem. 121 (2010) 233–237.
[22] M. Zhou, X. Chen, Y. Xu, J. Qu, L. Jiao, H. Zhang, H. Chen, X. Chen, Dyes Pigments 99 (2013) 120–126.
[23] A.P. Craig, A.S. Franca, J. Irudayaraj, Annu. Rev. Food Sci. Technol. 4 (2013) 369–380.
[24] J. Chen, J. Abell, Y.W. Huang, Y. Zhao, Lab Chip 12 (2012) 3096–3102.
[25] H. Xu, J. Aizpurua, M. Käll, P. Apell, Phys. Rev. E 62 (2000) 4318.
[26] J. Zheng, L. He, Comp. Rev. Food Sci. Food Safety 13 (2014) 317–328.
[27] J. Steidtner, B. Pettinger, Phys. Rev. Lett. 100 (2008) 236101.
[28] R. Zhang, Y. Zhang, Z.C. Dong, S. Jiang, C. Zhang, L.G. Chen, L. Zhang, Y. Liao, J. Aizpurua, Y. Luo, J.L. Yang, J.G. Hou, Nature 498 (2013) 82–86.
[29] S. Feng, F. Gao, Z. Chen, E. Grant, D.D. Kitts, S. Wang, X. Lu, J. Agric. Food Chem. 61 (2013) 10467–10475.
[30] Y. Hu, S. Feng, F. Gao, E.C. Li-Chan, E. Grant, X. Lu, Food Chem. 176 (2015) 123–129.
[31] F. Gao, S. Feng, Z. Chen, E.C. Li-Chan, E. Grant, X. Lu, J. Food Sci. 79 (2014) N2542–N2549.
[32] C.E. Freye, N.A. Crane, T.B. Kirchner, M.J. Sepaniak, Anal. Chem. 85 (2013) 3991–3998.
[33] C.L. Brosseau, A. Gambardella, F. Casadio, C.M. Grzywacz, J. Wouters, R.P. Van Duyne, Anal. Chem. 81 (2009) 3056–3062.

[34] K. István, G. Keresztury, A. Szép, Spectrochim. Acta A Mol. Biomol. Spectrosc. 59 (2003) 1709–1723.
[35] X. Lu, D.R. Samuelson, Y. Xu, H. Zhang, S. Wang, B.A. Rasco, J. Xu, M.E. Konkel, Anal. Chem. 85 (2013) 2320–2327.
[36] X. Lu, B.A. Rasco, D.H. Kang, J.M.F. Jabal, D.E. Aston, M.E. Konkel, Anal. Chem. 83 (2011) 4137–4146.
[37] T. Zhang, F. Liu, W. Chen, J. Wang, K. Li, Anal. Chim. Acta 450 (2001) 53–61.
[38] J.D. McGhee, P.H. von Hippel, J. Mol. Biol. 86 (1974) 469–489.
[39] Y. Zhao, X. Liu, D.Y. Lei, Y. Chai, Nanoscale 6 (2014) 1311–1317.
[40] C. Wang, F. Cheng, Y. Wang, Z. Gong, M. Fan, J. Hu, Anal. Methods 6 (2014) 7218–7223.
[41] J. Xue, D. Li, L. Qu, Y. Long, Anal. Chim. Acta 777 (2013) 57–62.
[42] D. Li, L. Qu, W. Zhai., J. Xue, J.S. Fossey., Y. Long, Environ. Sci. Technol. 45 (2011) 4046–4052.